The Use of Diamagnetically Levitated Silica Mirrors to Measure the Quantum Limit in Gravitational Wave Interferometry

Braeden Larson

July 31, 2024

Abstract

In this study, we explore the potential of diamagnetically levitated silica mirrors for measuring the quantum limit in gravitational wave interferometry. Conventional wire suspensions face limitations due to thermal noise at the 0.1 mg scale, making them unsuitable for achieving the standard quantum limit (SQL) in position measurement. Recent advances suggest that diamagnetic levitation could provide the necessary isolation from noise to investigate quantum decoherence at macroscopic scales. This research presents a simulation of a 3D magnetic field using a hybrid Finite Element Method Magnetics (FEMM) and MATLAB program to assess the feasibility of levitating highly reflective silica mirrors. The simulation results indicate that such mirrors can indeed be levitated, with optimization of the magnet system configuration identified. Additionally, an optical setup involving a piezoelectric feedback Michelson interferometer was constructed to further evaluate noise mitigation and achieve precise measurements. The experimental efforts and simulations are aligned with theoretical expectations and offer a promising approach to reaching the SQL in gravitational wave detection.

1 Introduction

There is a continued effort in gravitational wave research to find test masses that are insulated from noise. Furthermore, researchers in gravitational waves as well as other fields where highly precise measurement is important have begun to explore the idea that there might be some fundamental level of decoherence of quantum objects in the macroscopic world called gravitational decoherence in addition to decoherence objects face in their environment. Recently, it has been proposed that diamagnetically levitated mirrors would be best for insulating from common sources of noise to see this form of decoherence [5]. A crucial requirement for such experiments is achieving the standard quantum limit for position measurement sensitivity, which conventional wire suspensions cannot attain at the 0.1 mg scale due to thermal noise [5]. Researchers in the past have succeeded in the experimental verification to levitate unreflective 0.1-1 mg silica masses [5]. However, granted there is a lot of theoretical merit in these findings, refined and highly reflective silica itself has not yet been levitated successfully. To further aid research efforts, tests on the levitation height were simulated indicating that levitation of such mirrors is in fact possible using a hybrid FFEM and MatLab program to simulate a 3D magnetic field and sum over the average force experienced by a simulated silica mirrors with defined properties of density, permeability, and susceptibility. An optical cage setup aligned to a piezo locked Michelson interferomenter was also constructed and tested to mitigate noise from the mirrors in air.

2 Background

The primary objective for this project was to investigate the use of levitated silica mirrors to observe the limits of quantum noise. Hence, it is only natural to start at the definition of the quantum noise limit for unentangled or unsqueezed light, also known as the standard quantum limit.

First, to define a key lemma, consider this elegant derivation of Heisenburg's uncertainty principle using basic quantum mechanics. We start by considering a normalized wavefunction $\psi(x)$ such that $\lim_{x\to\pm\infty}\psi(x) = 0$ and $\lim_{x\to\pm\infty}\psi'(x) = 0$. The expectation values of position $\langle x\rangle$ and momentum $\langle p\rangle$ are given by

$$\langle x\rangle = \int_{-\infty}^{\infty} \psi^*(x)\, x\, \psi(x)\, dx$$

$$\langle p\rangle = \int_{-\infty}^{\infty} \psi^*(x) \left(-i\hbar \frac{d}{dx}\right) \psi(x)\, dx$$

In defining the wavefunction, we can always set ψ so that $\langle x\rangle = 0$ and $\langle p\rangle = 0$ since the wavefunction and its derivative go to zero at infinity (this is demonstrable by integration by parts and the use of the limit definition above). Hence, the uncertainties in position and momentum are

$$\langle \Delta x^2\rangle = \langle\psi|(x-\langle x\rangle)^2|\psi\rangle = \langle\psi|x^2|\psi\rangle = \langle x^2\rangle \text{ since } \langle x\rangle = 0$$
$$\langle \Delta p^2\rangle = \langle\psi|(p-\langle p\rangle)^2|\psi\rangle = \langle\psi|p^2|\psi\rangle = \langle p^2\rangle \text{ since } \langle p\rangle = 0$$

Furthermore,

$$\int_{-\infty}^{\infty} \left|\frac{d\psi}{dx}\right|^2 = \int_{-\infty}^{\infty} \frac{d\psi}{dx}\frac{d\psi^*}{dx} dx = -\int_{-\infty}^{\infty} \psi^* \frac{d^2\psi}{dx^2} dx \quad \text{(by integration by parts)}$$
$$= \frac{1}{\hbar^2}\int_{-\infty}^{\infty} \psi^* \hat{p}^2 \psi\, dx = \frac{1}{\hbar^2}\langle p^2\rangle = \frac{\Delta p^2}{\hbar^2}$$

Consider the non-negative integral

$$0 \le \int_{-\infty}^{\infty} \left|ax\psi + \frac{d\psi}{dx}\right|^2 dx$$

Expanding this, we get

$$0 \le \int_{-\infty}^{\infty} \left(a^2x^2|\psi|^2 + \left|\frac{d\psi}{dx}\right|^2 + ax\left(\psi^*\frac{d\psi}{dx} + \psi\frac{d\psi^*}{dx}\right)\right) dx$$

The term $ax\left(\psi^*\frac{d\psi}{dx}+\psi\frac{d\psi^*}{dx}\right)$ can be integrated by parts, along with the fact the wavefunction must be normalized, to give

$$a\int_{-\infty}^{\infty} x\left(\psi^*\frac{d\psi}{dx}+\psi\frac{d\psi^*}{dx}\right)dx = -a\int_{-\infty}^{\infty}|\psi|^2\,dx = -a$$

Thus, we have

$$0 \leq a^2\Delta x^2 + \frac{1}{\hbar^2}\Delta p^2 - a$$

where $\Delta x^2 = \langle x^2\rangle$ and $\Delta p^2 = \langle p^2\rangle$.

We consider the quadratic equation in a:

$$a^2\Delta x^2 + \frac{1}{\hbar^2}\Delta p^2 - a \geq 0$$

Solving for a, we find the discriminant must be non-negative,

$$(-1)^2 - 4\left(\Delta x^2\right)\left(\frac{1}{\hbar^2}\Delta p^2\right) \geq 0$$

$$1 - \frac{4}{\hbar^2}\Delta x^2\Delta p^2 \geq 0$$

Thus, we have derived the generalized uncertainty principle $\Delta x\Delta p \geq \frac{\hbar}{2}$. If $\Delta x\Delta p = \frac{\hbar}{2}$, we have by the definition of the integral

$$ax\psi + \frac{d\psi}{dx} = 0$$

This differential equation can be solved to give

$$\psi(x) = Ce^{-\frac{ax^2}{2}}$$

which corresponds to the ground state (zeroth order) of the quantum harmonic oscillator [3]

$$\psi(x) \propto e^{-\frac{x^2}{2\Delta^2}}e^{ip_0t/\hbar}$$

where $\Delta = \frac{1}{\sqrt{a}}$.

The reason for this rigor is because now we know that in order for a test mass to minimize its uncertainty in position as much as possible, assuming the position and momentum of itself are not entangled in some way, then it must obey the properties of the zeroth order quantum harmonic oscillator. The position operator of the test mass assuming it is a quantum harmonic oscillator can be written using raising and lowering operators [3] as follows

$$\hat{x} = \sqrt{\frac{\hbar}{2m\omega}}(a + a^\dagger)$$

where a and $a^\dagger$ are the annihilation and creation operators, respectively, $\hbar$ is the reduced Planck's constant, m is the mass of the particle, and ω is the angular frequency of the oscillator.

Using the properties of the raising and lowering operators [3], the zero point fluctuation (Δx_{zpf}) or the minimum uncertainty in position that the silica mirror can have can be derived as follows

$$\Delta x_{zpf} = \sqrt{\langle 0|\hat{x}^2|0\rangle - \langle 0|\hat{x}|0\rangle^2} = \sqrt{\langle 0|\hat{x}^2|0\rangle}$$

$$= \sqrt{\frac{\hbar}{2m\omega}\langle 0|a^2 + aa^\dagger + a^\dagger a + (a^\dagger)^2|0\rangle} = \sqrt{\frac{\hbar}{2m\omega}\langle 0|a^2 + aa^\dagger|0\rangle} = \sqrt{\frac{\hbar}{m\omega}}$$

From here, assume the measurement time is given as $\tau \approx \frac{1}{\pi f} = \frac{2}{\omega}$ and the power spectral density is given by $S_{SQL} = |\Delta x_{zpf}|^2\tau$.

Therefore, we have

$$S_{SQL} = \frac{2\hbar}{m\omega^2} = \frac{\hbar}{2m\pi^2 f^2}$$

This is the Standard Quantum Limit (SQL) of position. In a Michelson interferometer, the effective mass is considered as $\frac{m}{4}$ since the differential motion involves four mirrors. Additionally, we divide by L^2 (where L is the arm length) and take the square root to express the sensitivity in terms of strain. This leads to $S_{SQL}^{1/2}(f) = \frac{1}{2\pi f L}\sqrt{\frac{8\hbar}{M}}$. Other sources also derive this using the definitions of shot noise and radiation pressure [4]. This is because radiation pressure and shot noise are directly analogous to uncertainties from noise in position and momentum in the light itself hitting the mirror. The maximum allowable shot noise and radiation pressure are set equal to each other and the minimum noise is where they intersect, exactly at the SQL. This is the reason we are interested in diamagnetic mirrors. They are insulated from all noise in a theoretical perfect vacuum and potentially allow us to look at this noise directly, even having the ability to reach below the SQL using squeezed light.

Now that the basic objective of using silica mirrors is well defined, looking macroscopically, the basic idea behind implementation of diamagnetic levitation of a mirror test mass using classical magnetostatics for an assumed linearly magnetic silica is described as below [1, 2].

$$\mathbf{M} = \chi\mathbf{H}$$

$$\mathbf{B} = \mu_0(\mathbf{H} + \mathbf{M}) = \mu_0(1+\chi)\mathbf{H} = \mu\mathbf{H} \text{ assuming linear magnetic media}$$

$$\mathbf{M} = \frac{\mathbf{m}}{V} = -|\chi|\frac{\mathbf{B}}{\mu}$$

$$\mathbf{m} = -|\chi|\frac{\mathbf{B}}{\mu}V$$

$$F = \nabla(m \cdot B) \text{ (for further derivation, see [2])}$$

$$U = -m \cdot B$$

$$dU = -dm \cdot B + -dB \cdot m = -dm \cdot B$$

because the magnetic field does not change in a certain region, only the dipole.

$$U(z) = \int_0^{B(r)} -d\mathbf{m} \cdot \mathbf{B} = \int_0^{B(r)} -d(-|\chi|\frac{\mathbf{B}}{\mu}V) \cdot \mathbf{B} = \int_0^{B(r)} \frac{|\chi|V}{\mu}\mathbf{B} \cdot d\mathbf{B} = \frac{B^2\chi V}{2\mu}$$

$$U(z) = mgz + \frac{B(z)^2\chi V}{2\mu}$$

$$F(z) = -\frac{\partial U(z)}{\partial z} = -mg - \frac{\chi V}{\mu}\frac{\partial B(z)}{\partial z}B(z) = 0$$

$$\frac{\partial B(z)}{\partial z}B(z) = \frac{\mu\rho g}{\chi} \tag{1}$$

$$F(x_i) = -\frac{\partial U(x_i)}{\partial x_i} = -\frac{\chi V}{\mu}\frac{\partial B(x_i)}{\partial z}B(x_i) \text{ where } x_1 \text{ is x and } x_2 \text{ is y} \tag{2}$$

Equation 1 was used to check the conditions of the levitated mass for the program and find the levitation height of the mass over the magnet array at any x-y coordinate. Similarly, equation 2 was used to plot the horizontal forces of the mass, given it was at the stable levitation height determined by equation 1. The results of the simulation informed of the most optimal configurations of the system for levitation.

3 Methods: Program

This simulation was designed to mirror the physical apparatus used in our experiments by matching the geometry of the NdFeB magnet array and the levitated mirrors. By simulating the magnetic field distribution, the resulting forces, and the stability of the levitated mirror, we were able to estimate the variables of interest such as Q factor and levitation height while making necessary tweaks to the geometry of the system when necessary. Previous iterations of the code existed which analysed line segments of the magnets in 2D space – this idea was further developed by mapping the data in 3D space to more accurately represent the physical levitation setup as detailed below. The script uses a software called Finite Element Method Magnetics (FEMM) model, to simulate a setup for one ring, made of NdFeB with a strong magnetic field fixed inward toward the center (in real life made up of 8 strong, triangular magnets), surrounding an iron rod, as shown in Figure 1 below. The silica test mass attempted to be used was 0.6 mm tall with a diameter of 1.5mm. A test mass of similar size with a diameter of 1.5mm was also tested but was cut into a hemisphere with radius 0.75mm.

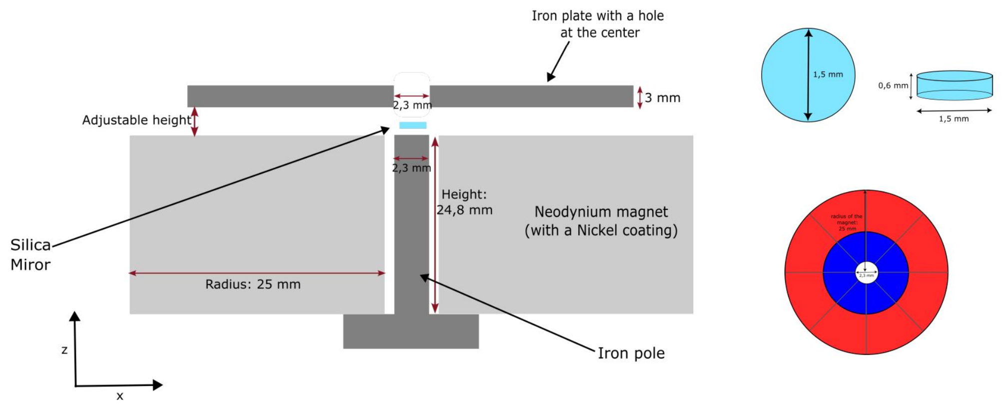

Figure 1: Diagram of Simulated Magnetic Array and Silica Test Mass

The script first defines dimensions for the simulation, such as the size of the air gap between the magnet and the iron rod, the thickness of the ring, and the material properties of both the silica and the magnets. It also initializes the geometry of the silica test mass and the magnet arrangement, setting up a detailed spatial model of the system centred around the z-axis to provide an accurate 3D description of the system. The magnets and the surrounding air regions are drawn and labelled within FEMM, as shown in Figure 2, and their properties are defined such as the ring magnet specifying a fixed magnetic field toward the center and the iron rod being made of pure iron. The simulation mesh is produced and analyzed to calculate the magnetic field components (B_r and Bz) at various points within the defined 2D space. These magnetic field data are then converted from a 2D axisymmetric model to a 3D cylindrical vector field by extending the 2D field data along the variable 'θ' direction, assuming rotational symmetry around the central axis as mentioned previously. Furthermore, the process of interpolating 2D points grid into a 3D grid that is axisymmetric limits computational efficiency heavily. The points created after the rotation must be equally spaced in order to be operated on effectively in a 3D Cartesian grid which takes time.

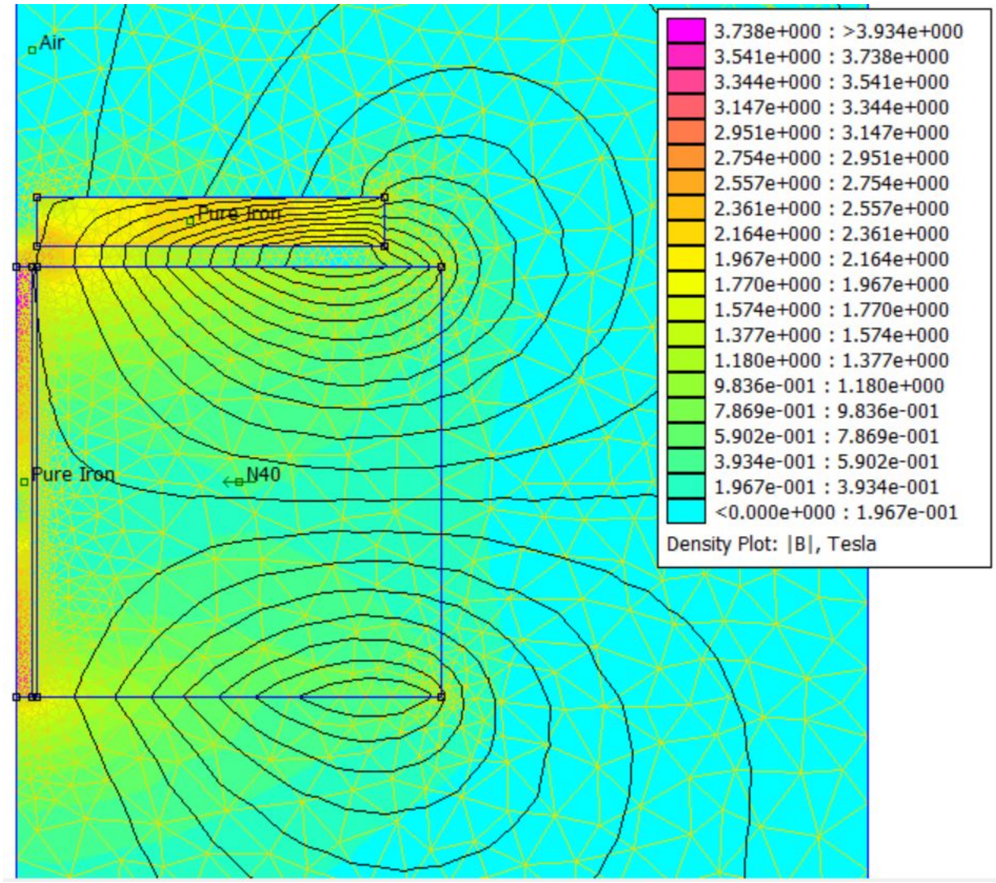

Figure 2: Simulated Magnetic Array Cross Section in 2D in FEMM

As shown in Fig 2, the 3D ring geometry is not explicitly defined in the 2D model as the initial calculation is to obtain the magnetic force vectors. The program then interpolates the magnetic field data onto a 3D grid and calculates the force components acting on the silica due to the magnetic field gradients. These calculations derive the average horizontal and vertical forces experienced by the silica mass. The script then verifies if the magnetic levitation force matches the gravitational force on the silica within a specified error margin (0.05e-5) according to Equation 1, ensuring that levitation conditions described previously are maintained. This is done by iterating through the z direction and calculating the difference between the gravitational force acting on the silica and the vertical force component due to magnetic field gradients (F_{bz}). The levitation height is incrementally adjusted until the difference meets a specified error threshold for the difference between the forces (0.05e-5) which ensures equilibrium. This process is by far the most computationally expensive segment of the program and imposes a hard limit on its accuracy by introducing a margin of error. The resulting matrix stores the calculated levitation heights across the 2D plane which is then plotted to provide a visual representation of levitation height. This is shown in Figure 3 with the results for levitation height of the system described in Figure 1 with a 1.2 mm distance between the iron plate, as was successful when researchers were first attempting to levitate silica [5].

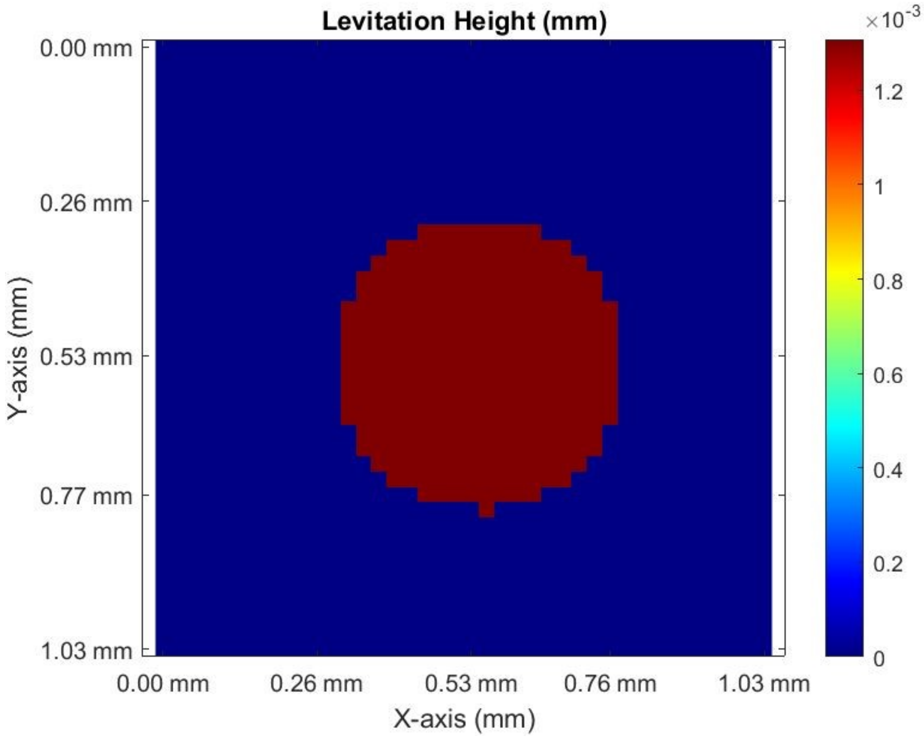

Figure 3: Diagram of Simulated Magnetic Array and Silica Test Mass

In practice, this program is used to determine the effectiveness of the system of magnets to levitate silica; if the levitation height is found to be insufficient or 0, changes can be made to the physical system of magnets to increase levitation height. At a reasonably low margin of error, the simulation states that macroscopic silica masses of up to 0.1g should passively levitate on the system of magnets constructed in the lab. As is shown in Figure 3, the current setup simulated seems sufficient enough to levitate the theoretical test mass at least 1.2mm.

4 Methods: Apparatus

In order to investigate the noise effects of levitating a silica test mass, a Michelson interferometer with a piezoelectric driver feedback was constructed to hook up to the magnetic array described in the previous section levitating a silica mass inside a vacuum. Several pieces of optical equipment from ThorLabs were ordered and assembled in order to cause a laser beam to focus vertically into the chamber as one arm of the interferometer, as shown in the figure below.

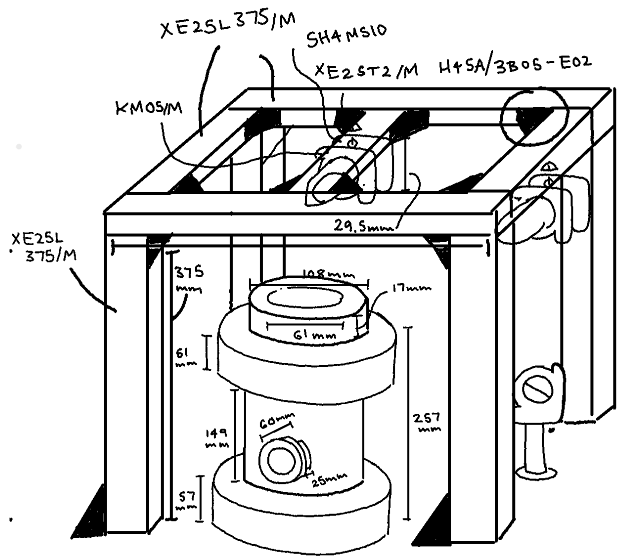

(a) Sketch of Cage Mount for Optics around Vacuum Chamber

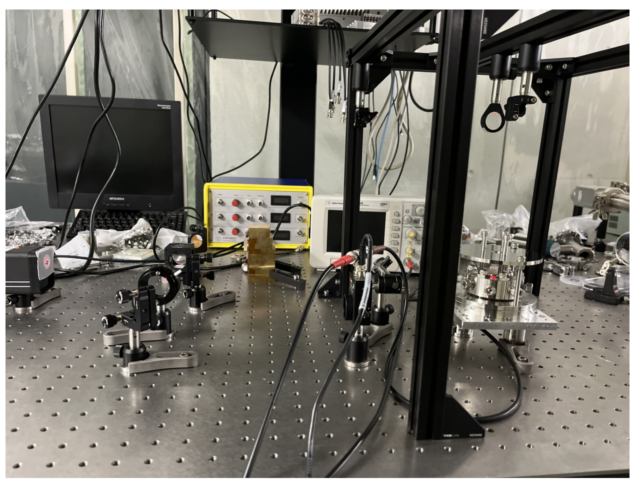

(b) Testing the Mount Outside the Vacuum Chamber to Align to the Piezoelectric Driver Glued to a Mirror (Attached on Gold Stand in Back) with a HeNe Laser

Figure 4: Setting Up the Vacuum Chamber Arm

The oscillations of the silica mirror should be isolated from movements of the other optical components as much as possible using a piezoelectric crystal attached to a mirror. Furthermore, the theory behind using a piezoelectric driver locked Michelson interferometer should be discussed in detail.

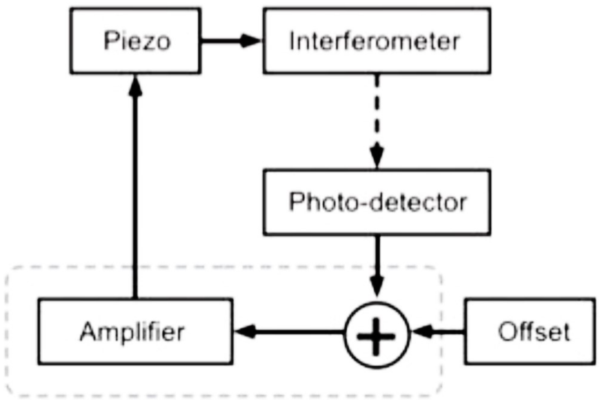

Figure 5: Simplified Diagram of Piezoelectric Feedback Loop

The general idea is as in the figure above. The interferometer gives an output signal at some fringe, say the mid-fringe, at a certain intensity that gives a certain offset in voltage from the photo-detector. This gets fed into a differential amplifier (signified by the plus and amplifier in the diagram) with an offset set to the same voltage that the mid-fringe from the interferometer gives. In this way, if the two signals are always the same, no voltage will be fed to the piezo and nothing happens. However, if there is a difference in the light recieved at the photodetector, the differential amplifier will give a non-zero difference between the output signal and the offset and the piezo will be driven until that difference is minimized. In this way, it is a feedback loop designed to minimize the variation in the mirrors outside the vacuum chamber [6].

In alignment as well, this setup of the piezoelectric driver also proved useful. If one drives a high voltage periodic signal through the piezoelectric crystal, one can clearly see oscillations in the fringe patterns, as shown in the figure below, if the system is aligned correctly.

Figure 6: Oscillations in the Fringes of the Michelson Interferometer (Yellow) given an Amplified Periodic Triangular Signal from Function Generator (Green)

In addition to this process of setting up the interferometer, levitation of the silica test mass was attempted.

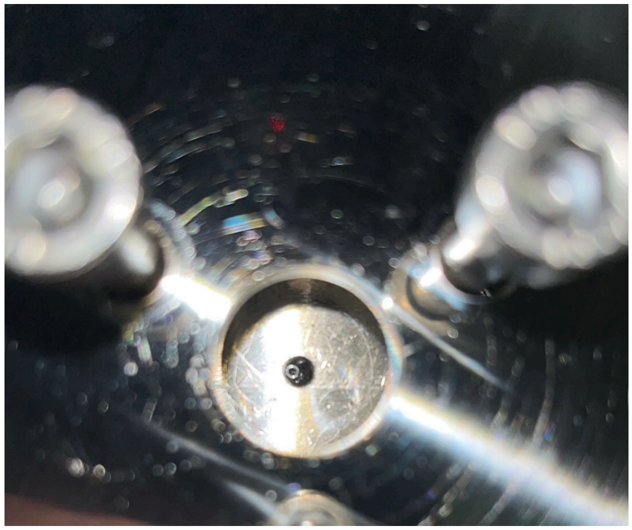

(a) Silica Mass Seemingly Levitating in the Magnetic Array

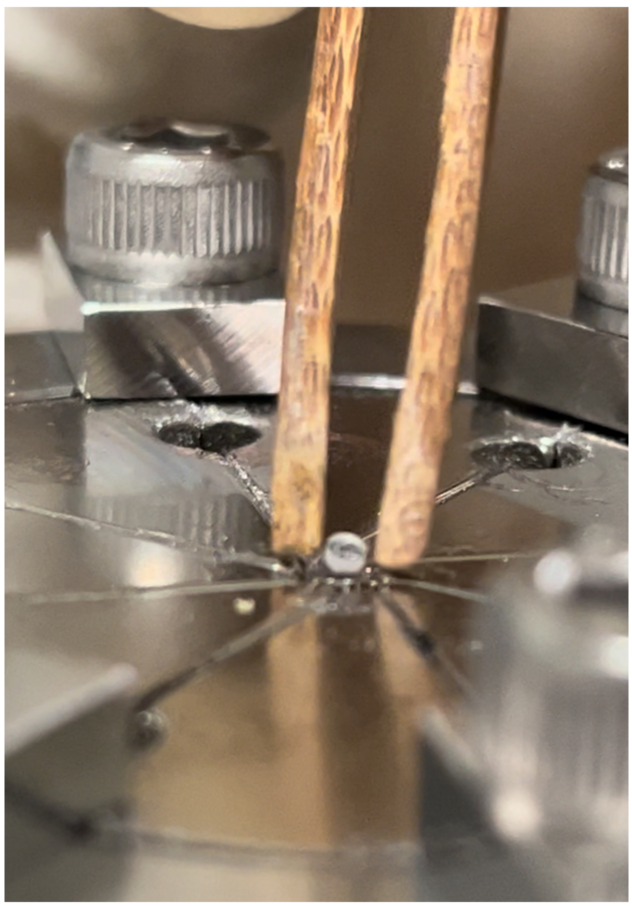

(b) Picking Up and Placing Silica Test Mass with Bamboo Tweezers

Figure 7: Levitating the Silica Test Mass

We attempted to levitate the silica test mass and align it to the interferometer. It could have been successful but we lacked the tools to properly see the silica under the iron plate and adjust it precisely. For the most part, we used wooden tools, since silica and other levitated masses, can acquire noise from static. Hence, we deionized the silica test masses before every attempt at levitation by holding it with tweezers over a deionizing fan. Slightly changing the heights of the iron plate and iron rod in the code seemed to cause better results in simulation and while testing the system, but we lacked the precision needed to be certain.

5 Conclusion

In this research, we have successfully constructed a piezoelectric driver for a Michelson interferometer and a simulation to inform whether the test masses were able to levitate and at what heights. Furthermore, we identified several potential problems with the levitation setup. Trial and error was used several times in adjustment of the magnetic array to levitate the silica and by the end of the two month period, we had surmised a configuration that seemed promising for future researchers to tweak more finely.

6 Future Work

Several suggestions have been made to improve specifically the levitation setup before accurate measurement of Q could be taken in the vacuum chamber. The most obvious, because the levitation height given our code was only at most 1mm, which is relatively difficult to see, is to use stronger magnets. We had been using N40 NdFeB magnets when there existed N52 magnets of stronger field that we were unaware of. Furthermore, the configuration of the triangular magnets were sliding past each other due to the air gap and not pointing directly toward the center, similar to the shape of an aperture, and we believe this was causing a circular field in real life around the iron rod which caused the silica mass to be forced outward from the center instead of inward. We attempted to adjust this through trial and error and observed much greater levitation heights.

7 Acknowledgements

I would like to thank everyone at the Somiya lab at the Tokyo Institute of Technology for helping me get adjusted and work on this project in Japan for the last two months. Particularly, Yuki Yamaguchi, Kaido Suzuki, and Ryo Iden were of great help. In addition, I would like to thank the other visiting researcher from Cardiff University for his support and determination that matched mine as we worked on this project together in Japan for two months, Maxwell Oliveira-Koudry. Finally, I would like to thank NSF and the University of Florida for the funding and the opportunity to research in Japan to work on a project like this, which has been a goal of mine for many years.

REFERENCES

[1] M V Berry and A K Geim. "Of flying frogs and levitrons". In: *European Journal of Physics* 18.4 (July 1997), p. 307. DOI: 10.1088/0143-0807/18/4/012. URL: https://dx.doi.org/10.1088/0143-0807/18/4/012.

[2] David J. Griffiths. *Introduction to Electrodynamics*. Boston: Pearson, 2013, pp. 268, 285.

[3] David J. Griffiths and Darrell F. Schroeter. *Introduction to Quantum Mechanics*. Third edition. Cambridge ; New York, NY: Cambridge University Press, 2018, pp. 31–37. ISBN: 978-1-107-18963-8.

[4] M. Maggiore. *Gravitational Waves: Volume 1: Theory and Experiments*. Gravitational Waves. OUP Oxford, 2008, pp. 516–523. ISBN: 9780198570745. URL: https://books.google.co.jp/books?id=AqVpQgAACAAJ.

[5] R. Nakashima. "Diamagnetic levitation of a milligram-scale silica using permanent magnets for the use in a macroscopic quantum measurement". In: *Physics Letters A* 384.24 (2020), p. 126592. ISSN: 0375-9601. DOI: https://doi.org/10.1016/j.physleta.2020.126592. URL: https://www.sciencedirect.com/science/article/pii/S037596012030459X.

[6] S. Shimoi. "Control of Michelson Interferometers and Introduction of Digital System". Graduation Thesis in 2016, Department of Physics, Somiya Laboratory. PhD thesis. Tokyo Institute of Technology, 2016. URL: https://www.gravity.phys.titech.ac.jp/doc/thesis/sotsuron_shimoi.pdf.